# Computation of Torque using different non-conforming Interface Techniques


1st Andreas Gschwentner
*Institute of Fundamentals and Theory in Electrical Engineering*
Graz, Austria

2nd Klaus Roppert
*Institute of Fundamentals and Theory in Electrical Engineering*
Graz, Austria

3rd Manfred Kaltenbacher
*Institute of Fundamentals and Theory in Electrical Engineering*
Graz, Austria


2022 IEEE 20th Biennial Conference on Electromagnetic Field Computation (CEFC) | 978-1-6654-6833-6/22/$31.00 ©2022 IEEE | DOI: 10.1109/CEFC55061.2022.9940668


***Abstract*—In this work, the influence of classical mortaring and Nitsche-type mortaring on the torque, calculated with the Maxwell stress tensor, is determined. The discretization of the air gap with quadrilateral and triangular elements as well as different non-conforming interface positions are investigated.**

***Index Terms*—electric drive, non-conforming mesh techniques, Maxwell stress tensor, induction machine, finite element method**


## I. Introduction

Due to environmental concerns, developing of energy- and resource-efficient electric motors is becoming increasingly important, especially in electromotive industry. For the design and analysis of electric machines, the finite element method is one of the most common tool for engineers. Nevertheless, considering the relative movement between stator and rotor as well as the torque computation are challenging and one of the key problems in the numerical analysis of electric machines.

Modeling movement can be computationally expensive. Restricted to geometrically simple moving conductor regions with constant velocity, the Minkowski transformation is a convenient approach [1]. The moving-band and the lock-stepping technique are methods based on a conforming mesh. The classical mortaring and Nitsche-type mortaring are techniques based on non-conforming interfaces (see, e.g. [2], [3] and [4]).

A various number of torque computation methods exist. The Maxwell stress tensor and Coulomb's method based on the principle of virtual work are typically used in finite element analysis. Generally, in Sadowski et al. [5] an overview and comparison of different methods are given. However, accuracy problems are reported for some torque computation methods. In [6] the dependency between different finite element discretization and the Coulomb's method as well as energy based methods using the moving band technique is investigated. The influence of conforming and non-conforming movement techniques on the Maxwell stress tensor method is shown in [7].

The focus of this paper is to investigate the influence of classical mortaring and Nitsche-type mortaring techniques on the Maxwell stress tensor method, considering quadrilateral and triangular finite elements in the air gap of the electrical machine as well as different non-conforming interface positions.

## II. Summary of used Methods

### A. Maxwell Stress Tensor

The torque computation using the Maxwell stress tensor method is given by the following relationship

$$\mathbf{T} = \mathrm{L} \int_{\Gamma} \left\{ \mathbf{r} \times \frac{1}{\mu_0} \left[ (\mathbf{B} \cdot \mathbf{n})\mathbf{B} - \frac{1}{2}\mathrm{B}^2 \mathbf{n} \right] \right\} \mathrm{d}\Gamma \,, \qquad (1)$$

with $\mathbf{T}$ the torque, $\mathrm{L}$ the length of the electric machine, $\mathbf{r}$ the distance between origin and midpoint of boundary-segment $\mathrm{d}\Gamma$, $\mu_0$ the permeability of vacuum, $\mathbf{B}$ the magnetic flux density and $\mathbf{n}$ the outward pointing normal vector of boundary-segment $\mathrm{d}\Gamma$.

### B. Classical Mortaring and Nitsche-type Mortaring

The basic formulation of the classical mortaring and Nitsche-type mortaring is illustrated on a 2D magnetostatic problem in the xy-plane. Therefore, the problem reads as

$$\begin{aligned} -\nabla \nu(\boldsymbol{x}) \nabla u &= J_{\mathrm{z}} \quad \text{in} \quad \Omega \\ u &= u_{\mathrm{e}} \quad \text{on} \quad \Gamma \,, \end{aligned} \qquad (2)$$

with $u$ the z-component of the magnetic vector potential $\mathbf{A} = (0, 0, u)^T$, $\nu$ the magnetic reluctivity and $J_{\mathrm{z}}$ the z-component of the current density.

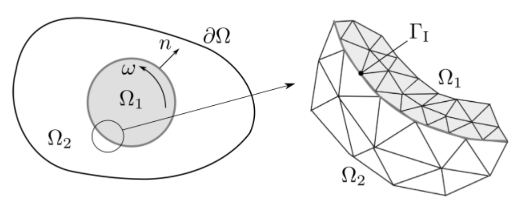


Fig. 1. Computational domain with the two subregions $\Omega_1$ and $\Omega_2$

*1) Classical Mortaring:* Classical mortaring adds additional degrees of freedom along the non-conforming interface in form of Lagrange multiplier $\lambda$, representing the primary unknown and the strong continuity condition along the interface is replaced by a weak one. Thus, (2) can be reformulated as

$$
\sum_{i=1}^{2} \left( \int_{\Omega_i} \nu_i(\boldsymbol{x}) \nabla u_i \cdot \nabla v_i \, \mathrm{d}\boldsymbol{x} - \int_{\Omega_i} J_{zi} \nabla v \, \mathrm{d}\boldsymbol{x} \right) + \int_{\Gamma_\mathrm{I}} [v] \lambda \mathrm{d}\boldsymbol{s} = 0 \qquad (3)
$$

$$
\int_{\Gamma_\mathrm{I}} [u] \mu \mathrm{d}\boldsymbol{s} = 0 \,,
$$

where $[]$ is the jump operator, defining the difference of the values across the interface.

*2) Nitsche-type Mortaring:* Nitsche-type mortaring incorporates essential boundary conditions weakly, symmetries the bi-linear form of the coupling and adds an additional penalization term for the jump of the primary unknown. In doing so, (2) reads as

$$
\begin{aligned}
&\int_{\Omega_1} \nu_1 \nabla v_1 \cdot \nabla u_1 \, \mathrm{d}\mathbf{x} + \int_{\Omega_2} \nu_2 \nabla v_2 \cdot \nabla u_2 \, \mathrm{d}\mathbf{x} \\
&- \underbrace{\int_{\Gamma_\mathrm{I}} \nu_1 [v] \frac{\partial u_1}{\partial \mathbf{n}} \, \mathrm{d}s}_{\text{Consistency}} - \underbrace{\int_{\Gamma_\mathrm{I}} \nu_1 \frac{\partial v_1}{\partial \mathbf{n}} [u] \mathrm{d}s}_{\text{Symmetrization}} \\
&+ \underbrace{\beta \bar{v} \sum_{E(\Gamma_\mathrm{I})} \frac{p_E^2}{h_E} \int_{\Gamma_E} [v][u] \mathrm{d}s}_{\text{Penalty/Stabilization}} \qquad (4) \\
&= \int_{\Omega_1} v_1 J_{z1} \, \mathrm{d}\boldsymbol{x} + \int_{\Omega_2} v_2 J_{z2} \, \mathrm{d}\boldsymbol{x}.
\end{aligned}
$$

## III. Simulation Model

In general, the simulation model is based on a 2D four pole squirrel cage induction motor. The air gap between rotor and stator is divided into four equidistant layers. Along the interface $\Gamma_\mathrm{maxwell}$ the torque computation using Maxwell stress tensor method is carried out. The non-conforming interface can be defined at either $\Gamma_\mathrm{NCinner}$ or $\Gamma_\mathrm{NCouter}$. For the regions $\Omega_\mathrm{outer}$ and $\Omega_\mathrm{inner}$, the mesh shown in Fig. 2 are used, where two different distortions of elements are defined. Overall, 8 different combination are investigated (see Tab. I).

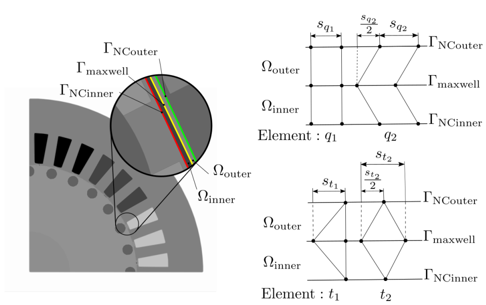


Fig. 2. Quarter model of a 2D four pole squirrel cage induction motor and quadrilateral and triangular mesh in the region $\Omega_\mathrm{outer}$ and $\Omega_\mathrm{inner}$

## IV. Preliminary Results

For all combinations in Tab. I, the torque is computed. Due to the non-moving rotor, the torque computation can also be performed with a conforming mesh. For the Nitsche-type method a Nitsche-factor of 2000 is chosen. Figure 3 shows the results using the classical mortaring and Nitsche-type mortaring compared to the results using a conforming mesh.

TABLE I
Different combination of elements and non-conforming interfaces

| ID | Element | NC-interface | ID | Element | NC-interface |
|---|---|---|---|---|---|
| 1 | $q_1$ | $\Gamma_\mathrm{NCinner}$ | 5 | $t_1$ | $\Gamma_\mathrm{NCinner}$ |
| 2 | $q_1$ | $\Gamma_\mathrm{NCouter}$ | 6 | $t_1$ | $\Gamma_\mathrm{NCouter}$ |
| 3 | $q_2$ | $\Gamma_\mathrm{NCinner}$ | 7 | $t_2$ | $\Gamma_\mathrm{NCinner}$ |
| 4 | $q_2$ | $\Gamma_\mathrm{NCouter}$ | 8 | $t_2$ | $\Gamma_\mathrm{NCouter}$ |

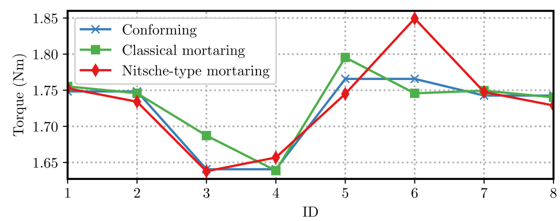


Fig. 3. Torque for different combinations based on the ID's from Tab. I

## V. Outlook

As shown in Fig. 3, the torque depends on a variety of factors. Therefore, the following will be investigated in further work. A convergence study to determine the influence of different Nitsche-factors as well as the influence of the discretization of the air gap. Furthermore, more detailed studies on the placement of the non-conforming interfaces as well as the node ratio between master and slave side. With the results obtained, further investigations with moving rotors will be carried out, which heavily involves non-conforming interfaces.

## References


[1] D. Rodger, "Modeling Movement in Electrical Machines", IEEE Transactions on Magnetics, Institute of Electrical and Electronics Engineers (IEEE), 2021, Vol. 57(6), pp. 1-4

[2] K. Roppert, S. Schoder, M. Kaltenbacher and F. Toth, 2018, "Non-conforming Finite Elements", International Compumag Society Newsletter, Jg. 2018, Nr. 3.

[3] K. Roppert, S. Schoder, G. Wallinger and M. Kaltenbacher, "Sliding Non-Conforming Interfaces for Edge Elements in Eddy Current Problems", IEEE Transactions on Magnetics, Institute of Electrical and Electronics Engineers (IEEE), 2021, Vol. 57(3), pp. 1-6

[4] G. J. Wallinger and O. Biro, "Improved Coupling Strategy to Cover Curved FE-Facets in the Non-Conforming Mesh Method", IEEE Transactions on Magnetics, Institute of Electrical and Electronics Engineers (IEEE), 2019, Vol. 55(6), pp. 1-4

[5] N. Sadowski, Y. Lefevre, M. Lajoie-Mazenc and J. Cros, "Finite element torque calculation in electrical machines while considering the movement" IEEE Transactions on Magnetics, Institute of Electrical and Electronics Engineers (IEEE), 1992, Vol. 28(2), pp. 1410-1413

[6] B. Silwal, P. Rasilo, L. Perkkio, M. Oksman, A. Hannukainen, T. Eirola and A. Arkkio, "Computation of Torque of an Electrical Machine With Different Types of Finite Element Mesh in the Air Gap" IEEE Transactions on Magnetics, Institute of Electrical and Electronics Engineers (IEEE), 2014, Vol. 50(12), pp. 1-9

[7] O. Antunes, J. Bastos, N. Sadowski, A. Razek, L. Santandrea, F. Bouillault and F. Rapetti, "Torque calculation with conforming and nonconforming movement interface" IEEE Transactions on Magnetics, Institute of Electrical and Electronics Engineers (IEEE), 2006, Vol. 42(4), pp. 983-986